

Upgrades and characterization of the Texas A&M quadrupole triplet spectrometer (QTS)

A.B. McIntosh, L. Heilborn, M. Youngs, L.A. Bakhtiari, M. Chapman, A. Jedele, L.W. May,
E. McCleskey, A. Zarrella, and S.J. Yennello

The Quadrupole Triplet Spectrometer (QTS) [1] used in conjunction with FAUSTUPS [2-4] promises to be a powerful tool for studying low and intermediate energy heavy ion reactions. This report describes upgrades of the detector suite and the achieved results. Since the status of FAUSTUPS is being described elsewhere [4], this report will focus on the QTS detectors. The upgraded FAUSTUPS-QTS system is ready for experiments beginning this summer 2015 to measure fusion-evaporation reactions.

The upgraded QTS detector suite is designed to measure four essential pieces of information for heavy residues produced near $\theta=0^\circ$: the energy (E), the velocity (V), the atomic number (Z) and the mass number (A). To access this information, three measurements are necessary: the time-of-flight (TOF), the energy loss in a thin passage detector, and the remaining energy in a stopping detector. The addition of the dE measurement since prior experiments is critical to understanding and discriminating atomic processes from nuclear reactions.

The TOF is measured using two XY position sensitive PPACs (Parallel Plate Avalanche Counters), one on either end of the QTS magnets. Additionally, plastic scintillators can be inserted into the line to provide timing information for less ionizing particles (light and fast products). In our recent experiment, the results of which are shown below, we demonstrated that $^{86}\text{Kr} + \text{C} @ 35 \text{ MeV/nucleon}$ and its reaction products are sufficiently heavily ionizing that the downstream PPAC provides reliable timing signals at the standard operating pressure of 6Torr and voltage of +530V. The dE-E measurement can be made with a thin silicon detector (58um) and a thick silicon detector (1000um). These two detectors comprise the Downstream Stack (DS).

The first data obtained using the full upgraded QTS suite including the dE information was obtained in run 041715 where the reaction system was $^{86}\text{Kr} + \text{C} @ 35 \text{ MeV/nucleon}$. Fig. 1 shows data obtained in the QTS detectors using the downstream (DS) stack as the trigger with the spectrometer tuned to 1.81Tm (84% of the rigidity of the beam) where fusion residues are expected to be found. A good signal in the three quantities is required: dE, E and TOF. The upper left panel shows the dE-E correlation. The elastic peak is clearly visible. Emanating from this peak are three rays of data. The long ray extending toward higher E and lower dE is consistent with channeling in the dE detector. The component tending to higher dE and lower E and having the same slope as the channeling component may be due to positive energy straggling in the dE. The component extending to lower E and constant dE is due to incomplete charge collection. A distribution of Z is visible at lower energies, consistent with fusion residues. At lower energy still is a thin band for only Z=36. A process that produces particles exclusively with the atomic number of the beam is an atomic process (i.e. slit scatter) rather than a nuclear process. The most likely edge for slit scatter is the Faraday cup just upstream of the QTS used to block unreacted beam inside of $\theta=0.9^\circ$.

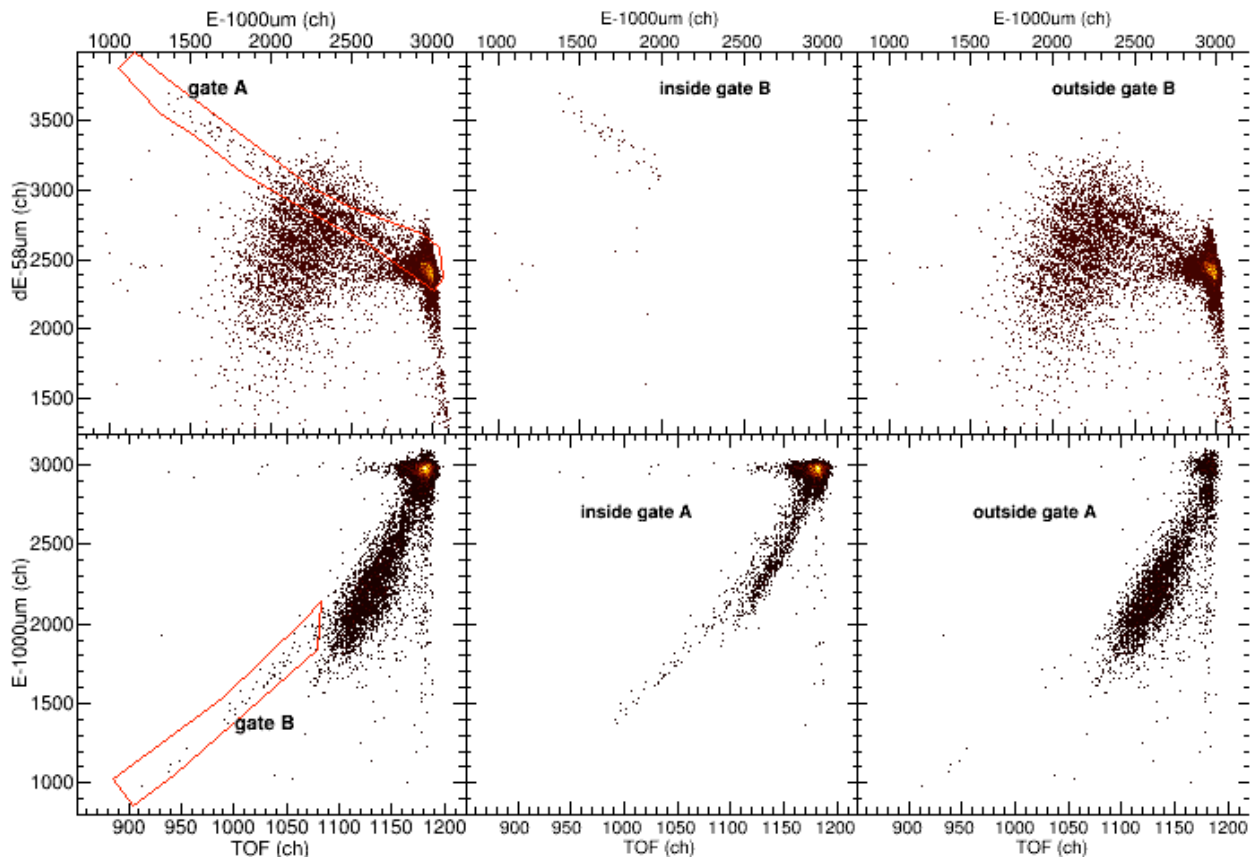


FIG. 1. Data from QTS detector array at $B\rho=1.81\text{Tm}$ with the downstream dE-E stack as the trigger. The top row shows dE-E correlations, which are sensitive to atomic number. The bottom row shows E-TOF correlations, which are sensitive to the mass number. The deviation of the residue band from the slit scatter band in the bottom middle indicates a decrease in the mass of the $Z=36$ residues with decreasing kinetic energy.

In the lower left panel of Fig. 1, the E-TOF correlation is shown. Short flight times appear on the right and longer flight times appear farther to the left. A significant distribution extends down from the elastic peak to about half the beam energy. A thin curve again extends through this yield and to lower energy still. To demonstrate the matching features between the two plots, a gate (B) is made on the thin curve in the E-TOF map. The dE-E map for data inside this gate is shown in the middle top panel; the data outside the gate is shown in the top right panel. The long thin curve in the E-TOF map is clearly associated with the long thin $Z=36$ band in the dE-E map, again consistent with slit scatter.

To further characterize the processes producing particles measured in the QTS detector suite, a gate (A) was defined around the $Z=36$ data in the dE-E map in the top right panel of Fig. 1. The E-TOF correlation for data inside (A) is shown in the bottom middle panel, and outside in the bottom right. The data outside the gate behaves as expected and does not exhibit the long slit scatter curve. The elastic peak is strongly suppressed, though remnants of the elastic peak exist. Most of the fusion residues in the E-TOF distribution lie outside the $Z=36$. Inside the $Z=36$ gate, we observe a high yield of the elastic peak, the long thin curve of slit scatter, and single narrow

band extending from the elastic and slightly sloping away from the slit scatter band. The slit scattered particles must have a constant mass of $A=86$. For $Z=36$ residues produced in nuclear reactions, the mass is not restricted to $A=86$. Higher masses are possible, but less likely since ^{86}Kr is already relatively neutron rich. Lower masses are possible and become increasingly likely with increasing excitation energy and thus increasing particle emission. In fact, this is what is observed – with increased kinetic energy loss, the residue distribution shifts to longer times than the slit scatter, implying a decreased residue mass. This is the first demonstration that the mass sensitivity that the QTS detector suite is expected to provide, and upon which we rely, is indeed realized.

Fig. 2 shows further data from the QTS detector suite also for $B_p=1.81\text{Tm}$ with FAUSTUPS CsI as the trigger. The requirement of a signal in FAUSTUPS strongly favors nuclear reactions over atomic interactions: the slit scatter line is gone and the elastic peak is highly suppressed as seen in the top left panel (dE-E) and the top right (E-TOF). Z identification

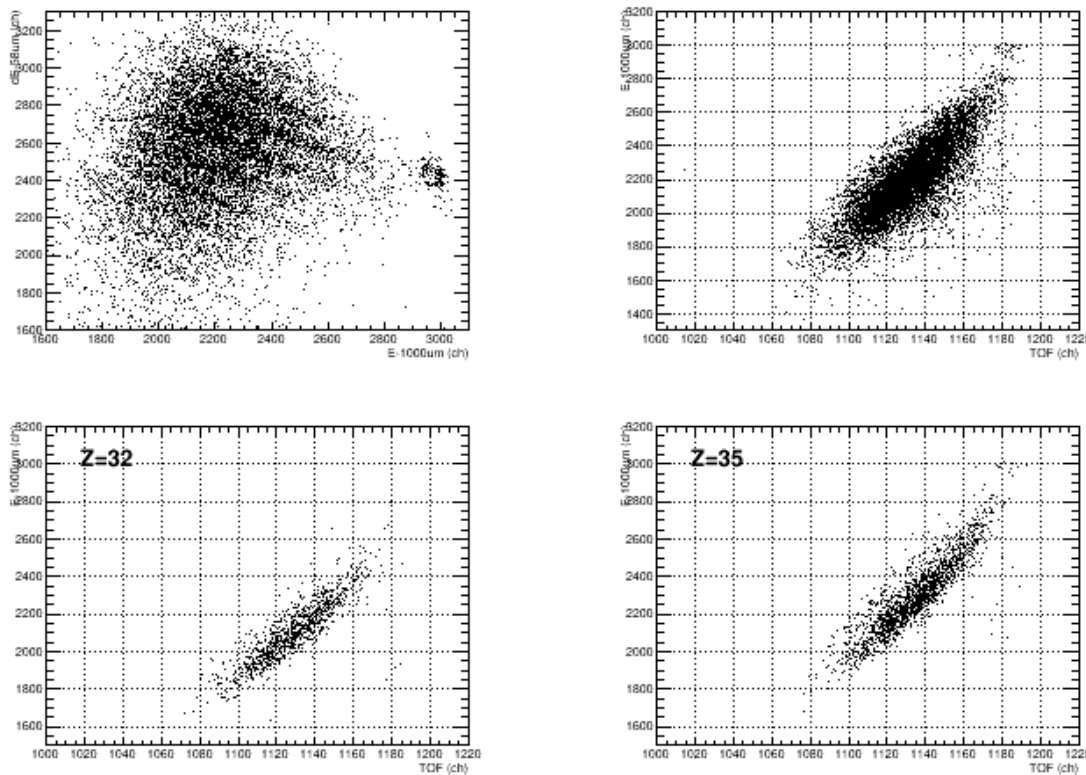


FIG. 2. Data from the QTS detector suite at $B_p=1.81\text{Tm}$ with FAUSTUPS CsI as the trigger. Slit scatter and elastic scatter are very strongly suppressed when FAUSTUPS is the trigger. Different Z are observed to populate different regions of the E-TOF map, further demonstrating the mass sensitivity of the QTS detector suite.

is achieved trivially from the dE-E map.

The lower two panels of Figure 2 display the E-TOF distribution for particles identified in the dE-E map as $Z=32$ (left) and $Z=35$ (right). The TOF range (and thus velocity) for the two

species are rather similar, while the $Z=35$ exhibits a significantly higher total energy than the $Z=32$ indicating significantly higher masses for $Z=35$ than for $Z=32$. This is the second demonstration of the mass sensitivity of the QTS detector suite. These two distributions are representative: for all atomic numbers identified, the velocity is not significantly affected by Z while the energy shifts to higher values with increasing Z .

This demonstrates that the QTS provides a clear method of separating atomic processes from the nuclear reactions of interest, and provides the information to characterize the nuclear residues in terms of Z , A , E , and V .

- [1] P. Cammarata *et al.*, Nucl. Instrum. Methods Phys. Res. **A** (accepted).
- [2] F. Gimeno-Nogues *et al.*, Nucl. Instrum. Methods Phys. Res. **A399**, 94 (1997).
- [3] S.N. Soisson *et al.*, Nucl. Instrum. Methods Phys. Res. **A613**, 240 (2010).
- [4] L.A. Heilborn *et al.*, *Progress in Research*, Cyclotron Institute, Texas A&M University (2014-2015), p. IV-54.